Exp.-Nr. **A2-10/09**
Eingang: 15.05.2009
an PAC: 18.05.2009

# Mainz Microtron MAMI

**Collaboration A2:** "Tagged Photons"
Spokesperson: A. Thomas

**Proposal for an Experiment**

## Measurement of Polarized Target and Beam Asymmetries in Pion Photo-Production on the Proton: Test of Chiral Dynamics

**Spokespersons for the Experiment :**
M. Ostrick - Mainz, D. Hornidge - Mt. Allison,
W. Deconinck, A.M. Bernstein - M.I.T.

**Abstract of Physics :**
We propose to perform precise measurements of the $\vec{\gamma}\vec{p} \to \pi^0 p$ reaction from threshold to partway up the $\Delta$ resonance using polarized beams and targets. These measurements will provide an additional, stringent test of our current understanding that the pion is a Nambu–Goldstone boson due to the spontaneous chiral symmetry breaking in QCD. Specifically we will test detailed predictions of chiral perturbation theory (ChPT) and its energy region of convergence. This experiment will test strong isospin breaking due to the mass difference of the up and down quarks. The data on the (time reversal odd)transversely polarized target asymmetry $\mathbf{T} = \mathbf{A}(\mathbf{y})$ will be sensitive to the $\pi$N phase shifts and will provide information for neutral charge states($\pi^0 p, \pi^+ n$) in a region of energies that are not accessible to conventional $\pi$N scattering experiments. The data on the double polarization observable $F = A(\gamma_c, x)$ (circular polarized photons-transverse polarized target) will be sensitive to the $d$-wave multipoles, which have recently been shown to be important in the near threshold region.

**Abstract of Equipment :**
We require a beam of tagged, circularly polarized photons incident on a transversely polarized butanol target. The detector will consist of the Crystal Ball photon spectrometer in combination with TAPS as forward wall. The Glasgow tagging system and the polarized electrons will be utilized.

**MAMI Specifications :**

| | |
|---|---|
| beam energy | 380 MeV |
| beam current | $< 20$ nA |
| beam polarisation | polarized |

**Photon Beam Specifications :**

| | |
|---|---|
| tagged energy range | 100 - 353 MeV |
| photon beam polarisation | circularly polarized |

**Equipment Specifications :**

| | |
|---|---|
| detectors | Crystal Ball/TAPS |
| target | frozen spin butanol (transversly polarized) |

**Beam Time Request :**

| | |
|---|---|
| set–up/tests with beam | 50 hours (parallel with proposal A2/11-09) |
| data taking | 600 hours (parallel with proposal A2/11-09) |

**List of participating authors:**


- **Institut für Physik, University of Basel, Switzerland**
  I. Jaegle, I. Keshelashvili, B. Krusche, Y. Maghrbi, F. Pheron, T. Rostomyan, D. Werthmüller
- **Institut für Experimentalphysik, University of Bochum, Germany**
  W. Meyer, G. Reicherz
- **Helmholtz–Institut für Strahlen- und Kernphysik, University of Bonn, Germany**
  R. Beck, A. Nikolaev
- **Massachusetts Institute of Technology , Cambridge, USA**
  A. Bernstein, W. Deconinck
- **JINR, Dubna, Russia**
  N. Borisov, A. Lazarev, A. Neganov, Yu.A. Usov
- **School of Physics, University of Edinburgh, UK**
  D. Branford, D.I. Glazier, T. Jude, M. Sikora, D.P. Watts
- **Petersburg Nuclear Physics Institute, Gatchina, Russia**
  V. Bekrenev, S. Kruglov, A. Koulbardis
- **Department of Physics and Astronomy, University of Glasgow, UK**
  J.R.M. Annand, D. Hamilton, D. Howdle, K. Livingston, J. Mancell, J.C. McGeorge, I.J.D. MacGregor, E.F. McNicoll, R.O. Owens, J. Robinson, G. Rosner
- **Department of Astronomy and Physics, Saint Mary's University Halifax, Canada**
  A.J. Sarty
- **Kent State University, Kent, USA**
  D.M. Manley
- **University of California, Los Angeles, USA**
  B.M.K. Nefkens, S. Prakhov, A. Starostin, I.M. Suarez
- **MAX-lab, University of Lund, Sweden**
  L. Isaksson
- **Institut für Kernphysik, University of Mainz, Germany**
  P. Aguar-Bartolome, H.J. Arends, S. Bender, A. Denig, E.J. Downie, N. Frömmgen, E. Heid, O. Jahn, H. Ortega, M. Ostrick, B.Oussena, P.B. Otte, S. Schumann, A. Thomas, M. Unverzagt
- **Institut für Physik, University of Mainz, D**
  J.Krimmer, W.Heil
- **University of Massachusetts, Amherst, USA**
  P.Martel, R.Miskimen
- **Institute for Nuclear Research, Moscow, Russia**
  G. Gurevic, R. Kondratiev, V. Lisin, A. Polonski
- **Lebedev Physical Institute, Moscow, Russia**
  S.N. Cherepnya, L.V. Fil kov, V.L. Kashevarov

- **INFN Sezione di Pavia, Pavia, Italy**
  A. Braghieri, A. Mushkarenkov, P. Pedroni
- **Department of Physics, University of Regina, Canada**
  G.M. Huber
- **Mount Allison University, Sackville, Canada**
  D. Hornidge
- **Tomsk Polytechnic University, Tomsk, Russia**
  A. Fix
- **Physikalisches Institut, University of Tübingen, Germany**
  P. Grabmayr, T. Hehl, D.G. Middleton
- **George Washington University, Washington, USA**
  W. Briscoe, T. Morrison, B.Oussena, B. Taddesse, M. Taragin
- **Catholic University, Washington, USA**
  D. Sober
- **Rudjer Boskovic Institute, Zagreb, Croatia**
  M. Korolija, D. Mekterovic, S. Micanovic, I. Supek

# 1 Motivation

Threshold pion photo-production and the closely related process of $\pi$N scattering have long been recognized as fundamental processes [1, 2], arising from the fact that the pion is the Nambu–Goldstone boson of QCD [3]. A significant amount of experimental [4] and theoretical effort [5, 6] has been put into these reactions. Overall, the pion scattering and production experiments strongly support our underlying concept of the pion as a quasi Nambu–Goldstone boson, reflecting spontaneous chiral symmetry breaking in QCD [3]. Despite many successes, not all of the chiral predictions have been properly tested. The long-standing prediction of Weinberg [7] that the mass difference of the up and down quarks leads to isospin breaking in $\pi$N scattering (in addition to the electromagnetic contribution) is of special interest in chiral dynamics. This pioneering calculation has been followed up by more recent ChPT analyses of isospin breaking in $\pi$N scattering [8] and pionic atoms [9, 10] to analyze the beautiful experimental work in pionic H and D[11]. Very recently a new calculation of the $\pi - N$ scattering lengths has been reported which calculates the contribution of the electromagnetic and quark mass contributions[12]. This paper improves on previous calculations and includes,for the first time, the isospin breaking contributions to all of the $\pi N$ states. These isospin breaking effects are predicted to be at the few percent level[12]. The experiments that are being proposed here will also be at that level of accuracy.

It is possible to characterize the successes of low-energy $\pi$N, and of photo- and electro-pion production experiments as verifying that the pion is the approximate Nambu–Goldstone boson of QCD, and that its low-energy production and interactions vanish in the chiral limit $m_u + m_d \to 0$ [18]. With this experiment we propose to measure the $\vec{\gamma}\vec{p} \to \pi$N reaction with a transversely polarized target and circularly polarized photons, as an important step in studying the dynamic consequences of $m_d - m_u > 0$.

Early work with the low energy theorems of current algebra made predictions for the $s$-wave amplitudes for $\pi$N scattering [13] and for the N$(\gamma, \pi)$ reaction [14, 15]. Subsequently an effective-field theory for QCD called chiral perturbation theory (ChPT) was developed [3, 5, 6, 16, 17]. This is an expansion in momentum and pion (light quark) masses which are small compared to the chiral symmetry breaking scale of $\simeq 1\,\mathrm{GeV}$. Since the perturbation series is truncated at a finite order, the effect of the neglected higher order terms can be estimated to determine the theoretical error. The main point is that these calculations should be a close approximation to QCD, and that any discrepancy between ChPT theory and experiment which are larger then the estimated errors must be taken seriously since they could represent a possible failure of QCD.

QCD exhibits chiral symmetry when the light quark masses are set to zero in the Lagrangian (the chiral limit). The absence of mass-degenerate parity doublets in the spectra of hadrons suggests that this symmetry is spontaneously broken (or hidden). The symmetry is not lost but appears in the form of massless, pseudoscalar Nambu–Goldstone bosons. As the lightest hadron, the pion best approximates the ideal Nambu–Goldstone boson. In the chiral limit, where the light quark and pion masses approach zero, the pion would not interact with hadrons at low energies (*i.e.* the $s$-wave scattering lengths would vanish). In reality, the small masses make the low-energy interaction weaker than a typical strong interaction, but the interaction remains non-zero. The near-threshold interactions are important to measure since they are an explicit effect of chiral symmetry breaking and have been

calculated by ChPT. In the future, lattice gauge theory is expected to also make accurate predictions. Since the occurrence of the quasi Nambu–Goldstone bosons signifies spontaneous chiral symmetry breaking in QCD, their low-energy interactions with other hadrons, their electromagnetic production and decay amplitudes as well as their internal properties (*e.g.* radii, polarizabilities, decay) will serve as fundamental probes of the chiral structure of matter. These measurements, involving small cross sections and polarization observables, have presented longstanding technical challenges.

## 1.1 Previous Threshold Photo-Pion Experiments

Threshold $\gamma p \to \pi^0 p$ experiments with high duty cycle accelerators have been carried out at Mainz [19, 20, 21, 22] and Saskatoon [23, 24]. These experiments are technically demanding since the cross sections are low. This is closely linked to the fact that the $s$-wave amplitude vanishes in the chiral limit. The Mainz effort, using the Glasgow tagger, has produced the best results but has taken a series of experiments to build up to its present capability to detect the $\pi^0 \to \gamma\gamma$ decay mode. The first experiment [19] had a small detector. Then the larger TAPS array was deployed [20] with corresponding better results. The Saskatoon work employed a $4\pi$ detector, but with very poor angular resolution. These experiments measured the cross section for unpolarized photons and as a consequence were not able to measure all of the multipoles. A first experiment with linear polarized photons was performed with the TAPS detector [21]. However, due to the small solid angle coverage, the statistics were limited and all of the linear polarized photon asymmetry points $\Sigma$ were lumped into one energy. At this time these are the best available data. The cross section data was grouped in approximately 1-MeV bins. The upper half of the energy region data, with the ChPT calculations are shown in Fig. 1. The small errors that are shown are statistical only and do not include the $\simeq 5\%$ systematic uncertainty. The measured points for the photon asymmetry $\Sigma$ are shown in Fig. 2.

The experimental progress outlined here is paralleled by a theoretical effort in ChPT [25, 26]. The most recent published calculations were performed with Heavy Baryon ChPT to one loop, or $O(p^4)$. The calculated curves [26] are shown in Fig. 1 and Fig. 2 and are in good agreement with the data. There are five low energy constants which have been fitted to the data. These are a small number in comparison with the number of data points. In addition their values are in reasonable agreement with estimated values [26]. The values of these constants can in principle be calculated by lattice QCD, which would represent another stringent test. The good agreement with experiment represents a striking success for these ChPT calculations, which are based on the symmetry structure of QCD. This represents a serious test of our ability to perform accurate calculations and test QCD in the confinement region.

As striking as the agreement with the data is, further more stringent tests are possible and this is what we are proposing. These tests involve the measurement of polarization observables which provide more stringent tests of the dynamics. In particular observation of the time reversal odd observables, which involve transverse polarized targets, are sensitive to the $\pi$N scattering phase shifts and can be used as isospin conservation tests. Furthermore it is important to extend the energy region so that we can understand quantitatively where ChPT calculations start to become less accurate. An additional element that has recently

been shown to be important is the need to introduce the $d$-wave amplitudes surprisingly close to threshold [28]. As will be discussed below it is possible to determine these effects with the proposed experiment.

The improvements proposed here are made possible by two technical developments of the A2 collaboration. They are the introduction of the almost $4\pi$ Crystal Ball detector in addition to the TAPS forward wall, and the new polarized target which will allow for transverse polarization. The first threshold $\vec{\gamma}p \to \pi^0 p$ experiment with linearly polarized photons and using the Crystal Ball detector was performed in December 2008 [22]. The results are presently being analyzed. This previous experiment will complement the proposed experiment in two important ways. First, the use of a liquid hydrogen target allows for more accurate cross section measurements than a polarized target with its mixture of C, O, and H. Secondly, the polarized photon asymmetry $\Sigma$ as a function of photon energy will also improve the knowledge of the $s$- and $p$-wave multipoles. Together they will provide an accurate data base for the real parts of these multioles. The present proposal will directly measure the important imaginary parts, and therefore the phase.

There is only one modern $\gamma p \to \pi^+ n$ experiment in the near-threshold region [24]. It was performed at Saskatoon using neutron detection and is in good agreement with the predictions of the Kroll–Ruderman [14] including chiral corrections [27]. This experiment was limited to a measurement of the $s$-wave photo-pion multipole $E_{0+}$ and no results were obtained for the $p$ waves. To do this will require experiments with polarized beams. We are presently investigating the reaction channel to $\pi^+ n$ for this proposal.

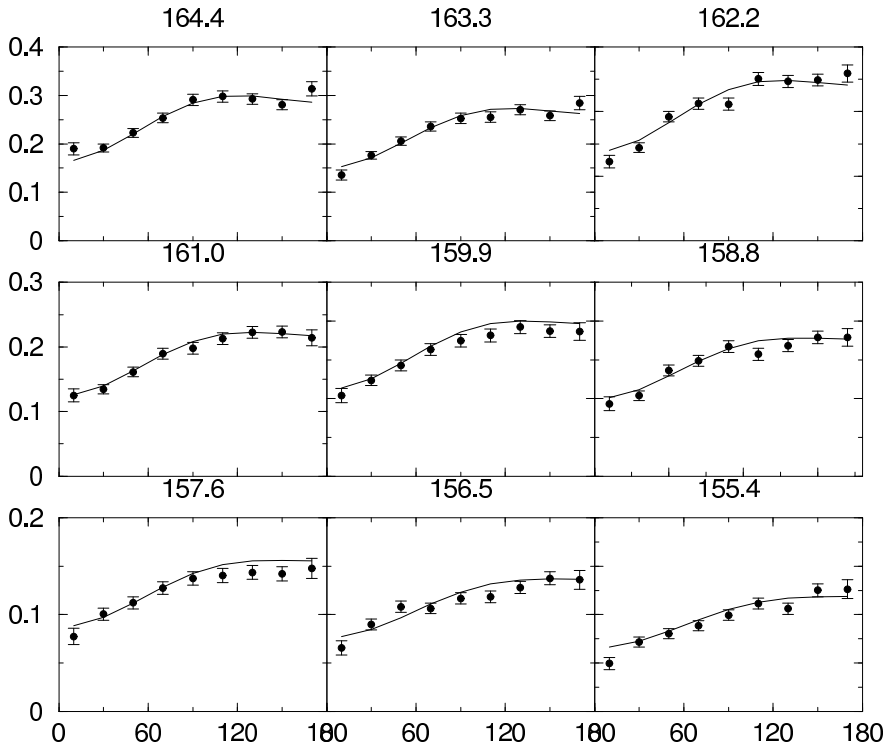


Figure 1: The cross sections versus the pion center-of-mass angle for the $\gamma p \to \pi^0 p$ reaction [21] with the ChPT calculation [25]. The error bars are statistical only and do not include the 5% systematic uncertainty. See the text for discussion.

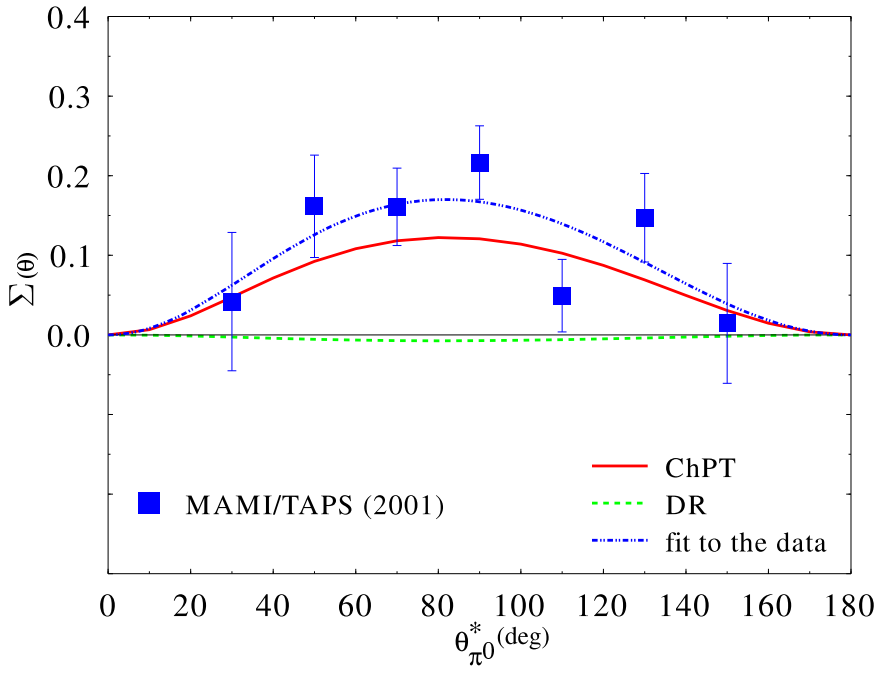


Figure 2: The experimental polarized photon asymmetry $\Sigma(\theta)$ versus the pion center-of-mass angle for the $\gamma p \to \pi^0 p$ reaction. These data are the cross section weighted asymmetries from threshold to 166 MeV at the average energy of 159.5 MeV [21]. The error bars are statistical only and do not include the 3% systematic uncertainty. The solid curve, labeled "ChPT," is an older [O($p^3$)] ChPT calculation [25]. The curve with the small dots, labeled "fit to the data," is a fit to the data and also is the same as the newer [O($p^4$)] ChPT calculation [26] with several new low energy parameters. See the text for discussion.

## 1.2 Photo-Pion Reactions and $\pi$N Scattering

The proposed experiment will have a major impact on another key area of low-energy QCD, namely $\pi$N scattering. From the measurement of the polarized target asymmetry $T$ just above the $\pi^+ n$ threshold we will be able to extract the charge exchange scattering length $a_{cex}(\pi^+ n \to \pi^0 p)$. With the exception of pionic atoms, the low energies of the threshold photo-pion experiments cannot be reached at conventional pion scattering facilities because the charged pion beams decay and one cannot make neutral pion beams at any energy. Moreover, the charge states involved here are different than in pion scattering experiments, which involve $\pi^{\pm} p$ elastic scattering and $\pi^- p \to \pi^0 n$ charge exchange.

An important ingredient in this measurement is the occurrence of a unitary cusp in the $s$-wave multipole $E_{0+}$. This occurs because the thresholds for the $\gamma p \to \pi^0 p$ and $\gamma p \to \pi^+ n$ reactions differ (an explicit isospin breaking effect). The dominant contribution to $E_{0+}(\pi^0 p)$ comes from the two-step reaction $\gamma p \to \pi^+ n \to \pi^0 p$, shown schematically in Fig. 3. The large magnitude of $E_{0+}(\gamma p \to \pi^+ n)/E_{0+}(\gamma p \to \pi^0 p) \simeq -20$ [25] drives the re-scattering effect responsible for the large magnitude of the cusp.

The equations, which are a generalization of the Fermi–Watson theorem [29] by removing the requirement of isospin conservation, have been derived using a 3 coupled-channel $S$

matrix approach in which unitarity and time reversal invariance are satisfied [30, 31]. This has the advantage that both static and dynamic isospin breaking, and multiple scattering in the final state (to all orders), are taken into account. The equation governing the unitary cusp is

$$\begin{aligned} E_{0+} &= e^{i\delta_0}[A_0 + i\beta q_+] \ ; \ \mathrm{W}{>}\mathrm{W}_{thr}(\pi^+\mathrm{n}) \\ E_{0+} &= e^{i\delta_0}[A_0 - \beta|q_+|] \ ; \ \ \mathrm{W}{<}\mathrm{W}_{thr}(\pi^+\mathrm{n}) \\ \text{where} & \\ \beta &= E_{0+}(\gamma p \to \pi^+ n) \cdot a(\pi^+ n \to \pi^0 p) \end{aligned} \tag{1}$$

Here $\beta$ is the constant parameterizing the magnitude of the cusp, and $a_{cex}(\pi^+ n \to \pi^0 p)$ is the $\pi$N $s$-wave charge exchange scattering length, $q_+$ is the $\pi^+$ center-of-mass momentum and $A_0$ is $E_{0+}$ in the absence of the charge exchange re-scattering. Based on unitarity alone, one does not know anything about $A_0$ other than that it is a smooth function of energy. In the unitary fit shown in Fig. 4, $A_0$ was parameterized as a linear function of photon energy [**?**].

The expected value of $\beta$ can be calculated [30] on the basis of unitarity using Eq. 1. Note that the sign of $\beta$ is observable, not just its magnitude, and agrees with what is expected. The best experimental value of $a(\pi^- p \to \pi^0 n) = -(0.1205 \pm 0.0026)/m_\pi$[9] obtained from the observed width in the $1s$ state of pionic hydrogen and from the level shift in pionic deuterium[11]. To extract this value the isospin breaking in pionic deuterium, primarily due to the electromagnetic interaction, was calculated[9]. Assuming isospin is conserved, $a(\pi^+ n \to \pi^0 p) = -a(\pi^- p \leftarrow \pi^0 n)$. The latest measurement for $E_{0+}(\gamma p \to \pi^+ n) = 28.06 \pm 0.27 \pm 0.45$ [1] [24] (where the first uncertainty is statistical and the second is systematic) is in good agreement with the ChPT prediction of $28.2 \pm 0.6$ [27]. Using these experimental values and the relationship given above leads to a value of $\beta = 3.38 \pm 0.10$. On the other hand, the ChPT prediction (which does not satisfy unitarity) is $\beta = 2.78$ [25, 26]. This difference is due to the truncation of the ChPT calculation at the one-loop $O(q^4)$ level. Taking isospin breaking into account the theoretical value of $a_{cex}(\pi^+ n \to \pi^0 p) = 0.1182 \pm 0.0027$, a reduction of $1.9 \pm 0.7\%$. This isospin breaking effect in within the range of accuracy of this proposed experiment.

The value of $\beta$ presented here is at the $\pi^+ n$ threshold. For higher energies the value is proportional to the value of the $E_{0+}(\gamma p \to \pi^+ n; E_\gamma)$ amplitude (evaluated at photon energy $E_\gamma$) which is predicted to decrease slightly with increasing $E_\gamma$ [33].

An instructive meeting ground between theory and experiment are the electromagnetic multipoles. The experimental observables (cross sections and asymmetries) are bilinear products of the (complex) multipoles. The extraction of the multipoles is model dependent unless a complete experiment has been performed[35]. This requires experiments with polarized targets and recoil nuclei[35]. The present experiments are far short of this requirement so that the multipole extraction is model dependent. One of the assumptions that has been previously made for both theory and experiment is that in the near threshold region only s and p wave pion production is important. In a recent paper it was demonstrated that this was not true and that the d wave contribution significantly effected the extraction of the s wave multipole $E_{0+}$[28]. This was shown using the Born approximation for the magnitude of the d wave multipoles. The Born terms that were used are in agreement with those used in the ChPT calculations for the s and p waves[25, 26]. In this paper[28] a new

[1] The units for $E_{0+}$ and $\beta$ are $10^{-3}/m_\pi$, while for the scattering lengths are $1/m_\pi$.

fit to the data using the ChPT formalism[25, 26] but including the effect of the d waves. In this proposal we indicate a way that the effect of the d waves can be directly observed in the double polarization observable using circularly polarized photons and a transversely polarized target.

Recent results for $ReE_{0+}$ are presented in Fig. 4. The extracted points[28] are from the latest published Mainz data [21] including the d wave contribution. ChPT[25, 26] was used to fit the data assuming s and p waves (as in the original papers) and also taking the d wave contribution into account (sp and spd fits)[28]. The curves show the difference between the empirical analyses with the *spd* and *sp* fits. The difference between the two curves shows how important the $d$ waves are close to threshold, and that they must be taken into account to have an accurate extraction of the $s$-wave multipole $E_{0+}$. The third curve shows the latest unitary fit to the latest Mainz data [21]. The main point of this fit is that the value of $\beta$ is fixed to the unitary value of 3.4 instead of the ChPT value of 2.78. It can be seen that the difference between the unitary and spd curves is very small. The only way to accurately measure the value of $\beta$ is to determine $ImE_{0+}$ through a measurement of the transversely polarized target asymmetry $T$. This is the main objective of this proposal.

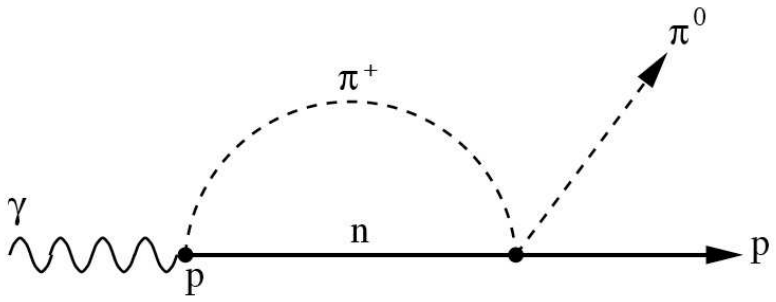


Figure 3: Rescattering diagram responsible for the unitary cusp observed in $E_{0+}(\gamma p \to \pi^0 p)$.

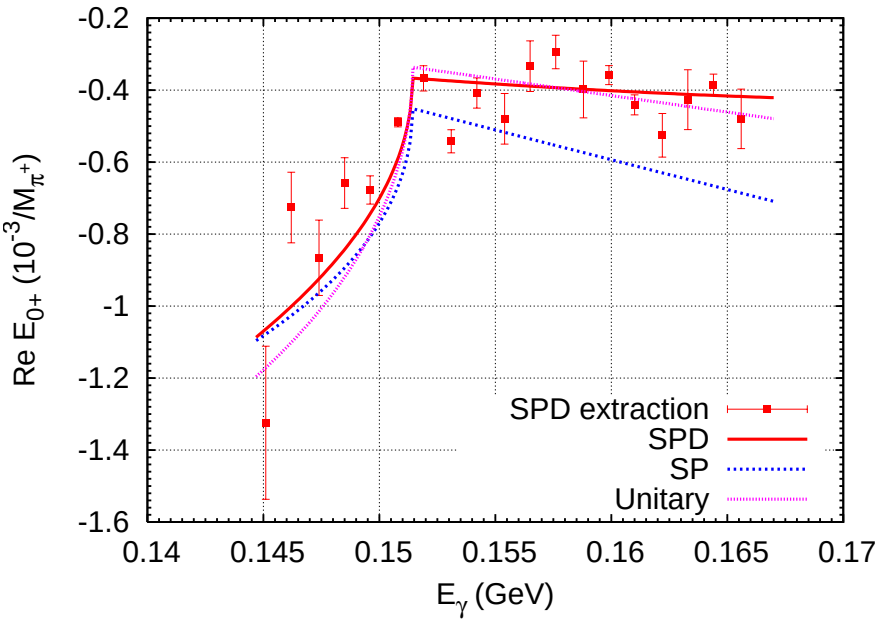


Figure 4: $ReE_{0+}(\gamma p \to \pi^0 p)$ versus photon energy. The curves are the ChPT calculations [26] with new low energy parameters using $s$ and $p$ waves, $sp$ and $d$ waves, and a unitary fit [28] to the data [21] for the low energy constants. The points were extracted from the data assuming sp and d waves contribute[28]. The error bars represent the statistical uncertainty only. See text for discussion.

# 2 Photoproduction Observables with Full Polarization

We are proposing measuring near threshold photo-pion production from a transverse polarized proton target using tagged, circularly polarized photons. For this case the differential cross section for pion photoproduction in the center-of-mass system has the form [34, 4]:

$$d\sigma/d\Omega_\pi \;=\; (p^*_\pi/k^*_\gamma)[R^{00}_T + P_x\Pi_\odot R^{0x}_{TT'} + P_y\boldsymbol{R^{0y}_T} + P_z\Pi_\odot R^{0z}_{TT'}] \tag{2}$$

where each $R$ is a response function (the response functions in boldface is time reversal odd), $p^*_\pi$ and $k^*_\gamma$ are the center-of-mass momenta of the pion and photon, respectively, $\varphi$ is the angle between the photon polarization vector and the reaction plane, $\Pi_\odot$ is the magnitudes of the photon's circular polarization on a scale from zero to one. The $P_{x,y,z}$ terms are the magnitudes of the target polarization in the $\pi$N center-of-mass reaction plane where $z$ is the photon direction, $x$ is transverse in the reaction plane, and $y$ is transverse and perpendicular to the reaction plane. $R^{00}_T$ is the unpolarized observable and $\boldsymbol{R^{0y}_T}$ is a single polarization observable. The notation denotes each response function for three different polarized target directions: $R^{0x}, R^{0y}$, and $R^{0z}$. The boldface symbol is a time reversal odd observables (TRO; imaginary parts of the bilinear products of the multipoles). The other response functions are time reversal even (TRE; real parts of the bilinear products of the multipoles). The TRO amplitude is crucial in measuring the phases of the amplitudes, which makes it sensitive to the $\pi$N physics. The different terms in Eq. 2 can be separated by their dependence on $\varphi$.

Equation 2 is in the center-of-mass (CM) system so we must Lorentz transform the observables from the laboratory system: this is taken as a right-handed coordinate system in which the photon direction is $z_L = z$, $x_L$ is transverse in the plane of the floor, and $y_L$ is transverse and perpendicular to the plane of the floor. In this lab system we define the pion direction as $\theta^L_\pi, \phi_\pi$, so that the orientation of the reaction plane is $\phi_\pi$ (the value of $\phi$ is the same in the lab and the CM system). When the photon polarization is chosen parallel to $x_L$, then $\varphi = \phi_\pi$; when it is parallel to $y_L$, $\varphi = \pi/2 - \phi_\pi$. The value of $\theta_\pi$ in the CM system is obtained from $\tan\theta_\pi = \beta_\pi \sin\theta_\pi/[\gamma_{CM}(\beta_\pi\cos\theta_\pi - \beta_{CM})]$, where $\beta_\pi = p_\pi/E_\pi, \beta_{CM} = k/(k+M_p), \gamma_{CM} = (1-\beta^2_{CM})^{-1/2}$ and $k$ is the photon energy in the lab system. We know the target polarization in the lab system where it has magnitude $p_T$, points in the direction $\theta_T, \phi_T$ and its four vector is $(0, \vec{P_T})$[35]. To obtain the target polarization in the CM system we have to perform another Lorentz transformation. As a consequence, the $z$ component is transformed. The transverse target polarization components remain the same in magnitude as in the lab system, $P_{xL} = P_T \sin\theta_T \cos\phi_T$ and $P_{yL} = P_T \sin\theta_T \sin\phi_T$. However, care must be taken in calculating $P_x, P_y$ since these coordinates are defined relative to the pion production plane which is at angle $\phi_\pi$ relative to the lab plane. In this frame the $y$ axis (normal to the reaction plane) is in the direction of $\hat{p^*_\pi} \times \hat{k}$ and $\hat{x} = \hat{y} \times \hat{k}$ where $p^*_\pi$ is the pion CM momentum. Therefore the target polarization in the CM frame is

$$\begin{aligned} P_x &= P_T \sin\theta_T \cos(\phi_T - \phi_\pi), \\ P_y &= P_T \sin\theta_T \sin(\phi_T - \phi_\pi), \\ P_z &= \gamma_{CM} P_T \cos\theta_T \end{aligned} \tag{3}$$

Note that if $\theta_T = 0$ the CM polarization is longitudinal, but is changed in magnitude. For a transverse target polarization ($\theta_T = 90^0$) the magnitude of the polarization is unchanged but note that an additional $\phi_\pi$ dependence is introduced.

| Observable | | Response Function | Name |
|---|---|---|---|
| $\sigma_T(\theta^*_\pi)$ | = | $(p^*_\pi/k^*_\gamma)R^{00}_T$ | Transverse Differential Cross Section |
| $A(\vec{\gamma}) \equiv \Sigma(\theta)$ | = | $-R^{00}_{TT}/R^{00}_T$ | Polarized Photon Asymmetry |
| $\boldsymbol{A(y) \equiv T(\theta)}$ | = | $\boldsymbol{R^{0y}_T/R^{00}_T}$ | Polarized Target Asymmetry |
| $A(\gamma_c, z) \equiv E(\theta)$ | = | $-R^{0z}_{TT'}/R^{00}_T$ | Circ. Photon - Long. Target |
| $A(\gamma_c, x) \equiv F(\theta)$ | = | $R^{0x}_{TT'}/R^{00}_T$ | Circ. Photon - Trans. Target |
| $\boldsymbol{A(\vec{\gamma}, z) \equiv G(\theta)}$ | = | $\boldsymbol{-R^{0z}_{TT}/R^{00}_T}$ | Trans. Photon - Long. Target |
| $\boldsymbol{A(\vec{\gamma}, x) \equiv H(\theta)}$ | = | $\boldsymbol{R^{0x}_{TT}/R^{00}_T}$ | Trans. Photon - Trans. Target |
| $\boldsymbol{A(\vec{\gamma}, y) \equiv P(\theta)}$ | = | $\boldsymbol{-R^{0y}_{TT}/R^{00}_T}$ | Trans. Photon - Normal Target |

Table 1: Observables for photo-pion production with polarized photons and targets [34]. The top line is the unpolarized cross section. All other entries are asymmetries. The second box contains the single polarization observables. The next group consists of the double polarization observables. The last entry can also be observed as the recoil polarization asymmetry. A new, more transparent notation is introduced here for the asymmetries (*e.g.* $\boldsymbol{A(\vec{\gamma}, y)}$), and the historical notation (*e.g.* $\boldsymbol{P(\theta)}$) is also presented. As throughout this proposal, the time reversal odd observables (imaginary bilinear combinations of multipoles) are indicated in boldface. Only six of the eight observables are independent [35].

Experimentally one usually measures asymmetries, which are generally obtained with more accuracy since they are less sensitive to normalizations than absolute cross sections. The seven asymmetries that can be obtained from the eight response functions are presented in Table 1. Here we introduce a new, more transparent notation as well as giving the historical one.

There is the important issue of how many partial waves are contributing. In the low energy regime it usually has been assumed that only the $s$- and $p$-wave multipoles are important. Then ; *e.g.* $\sigma_T = A_T + B_T \cos\theta + C_T \cos^2\theta$. If $d$ waves become sufficiently important then $\sigma_T = A_T + B_T \cos\theta + C_T \cos^2\theta + D_T \cos^3\theta + E_T \cos^4\theta$. In addition to the greater angular variation when $d$ waves are important, the numerical values of $A_T, B_T, C_T$ are not the same [28]. This simple example indicates the need to cover a sufficient angular range in each experiment and also sets requirements for the angular resolution and binning of the experiments.

We shall conclude this section by giving an example of how the multipoles have been extracted from the data at low energies. In the low energy region (below $\simeq 165\,\mathrm{MeV}$) it has been assumed that only $s$- and $p$-wave multipoles contribute and furthermore that the three $p$-wave multipoles are purely real (see *e.g.* Ref. [**?**, 21]). In this approximation (which must be checked with more accurate future data) five numbers must be determined, $ReE_{0+}, ImE_{0+}, P_1, P_2$, and $P_3$, where these three $p$-wave amplitudes are defined in terms of the usual multipole amplitudes by:

$$\begin{aligned} P_1 &= 3E_{1+} + M_{1+} - M_{1-} \\ P_2 &= 3E_{1+} - M_{1+} + M_{1-} \\ P_3 &= 2M_{1+} + M_{1-}, \end{aligned} \tag{4}$$

where $M_{1+}$ and $M_{1-}$ are the $p$-wave magnetic dipole amplitudes for $j = \frac{3}{2}$ and $\frac{1}{2}$, respectively,

and $E_{1+}$ is the $p$-wave electric quadrupole amplitude with $j = \frac{3}{2}$ [35]. From the measurement of $\sigma_T$ one obtains $A_T = |E_{0+}|^2 + 1/2(|P_2|^2 + |P_3|^2), B_T = 2Re(E_{0+}P_1^*)$, and $C_T = |P_1|^2 - 1/2(|P_2|^2 + |P_3|^2)$. The next step was taken at Mainz by the measurement of the polarized photon asymmetry [21] which determines $R_{TT}^{00} = 1/2(|P_2|^2 - |P_3|^2)\sin\theta^2$. This still leaves us one observable short of an experimental determination of all of the multipoles, even with the restricted assumptions.

The observable of choice is the time reversal odd polarized target asymmetry $\mathbf{R_T^{0y}} = \mathbf{T} = \sin\theta Im[((E_{0+}^* + \cos\theta P_1^*)(P_2 - P_3)] \rightarrow Im[E_{0+}(P_3 - P_2)]\sin\theta$ where the last line indicates that the $p$-wave amplitudes have been assumed to be real. From this equation we can obtain $ImE_{0+}$. It should be noted that if there is a contribution from higher partial waves or if the imaginary parts of the $p$-wave multipoles are not negligible, then there will be additional $\theta$ dependent terms in $\mathbf{R_T^{0y}}$. This can be experimentally tested with new data.

There are also two time reversal even asymmetries which are very large in the threshold region which can provide additional and precise measurements of the multipoles which will further test the assumptions on which the present data are analyzed. There are the two double polarization asymmetries induced with circular polarized photons: $A(\gamma_c, z) \equiv E(\theta)$ and $A(\gamma_c, x) \equiv F(\theta)$. In the $sp$-wave approximation the numerator of the latter is $R_{TT'}^{0x} = \sin\theta Re[(E_{0+}^* + \cos\theta P_1^*)(P_2 - P_3)]$. It can be seen that a measurement of the angle ($\theta_{F0}$, not 0 or 180°) for which this observable is zero provides an independent determination of $Re(E_{0+}^*) = -\cos\theta_{F0}Re(P_1)$. As will be discussed in the next section the value of $\theta_{F0}$ is altered by the presence of $d$ waves [28] and can be observed. Finally we note that in the $sp$-wave approximation $R_{TT'}^{0x}$ and $\mathbf{R_T^{0y}}$ are the real and imaginary parts of the same combination of the mutipoles. This is a very powerful combination to measure the $\pi$N phases.

# 3 Proposed Experiment

We propose to measure for the first time the polarized target asymmetry $A(y) \equiv T(\theta)$ and the double polarization asymmetry $A(\gamma_c, x) \equiv F(\theta)$ in the threshold region. Both asymmetries require a transversely polarized target, and the second asymmetry requires a circularly polarized photon beam. We plan to measure the reaction channel $\gamma p \to \pi^0 p$ in the energy region from threshold through approximately 250 MeV, part way up the $\Delta$ resonance. This will represent the completion of a long series of productive experiments on this reaction, particularly in combination with the recently completed polarized photon experiment using the Crystal Ball and the TAPS forward wall [22]. Although we also plan to investigate the $\pi^+ n$ channel, this proposal primarily focuses on the $\pi^0 p$ channel in the region from threshold to approximately 200 MeV.

## 3.1 Experimental Setup and Running Conditions

The A2 setup of the tagged photon beam, the crystal ball ,TAPS forward wall, and the polarized target are presented in the appendix. In this section we present the special requirements of this experiment.

With an electron beam energy $E_e = 450\,\mathrm{MeV}$, the tagged photon energy range will be $E_\gamma = 50 - 400\,\mathrm{MeV}$. this will cover the energy region we wish to investigate. The tagging efficiency in the region of interest should be around $\epsilon_{tag} = 0.25$ or higher. The electron count rate in the tagger is estimated as 0.5 MHz for each channel of 1 MeV wide, or $\dot{N}_e = 0.5\,\mathrm{MHz/MeV}$. We expect that the circular polarization will be $\Pi_\odot \approx 50\%$ or better, with an energy dependence as shown in Fig. 5. In can be seen from this figure that it is advantageous to use a lower beam energy in order to increase the magnitude of the circular polarization. Running at 450 MeV instead of 850 MeV means that our energy resolution per tagger channel is $\simeq$ 1 MeV/channel instead of 2 MeV, which is an advantage in measuring the energy dependence in the unitary cusp.

We intend to use the transversely polarized butanol target. The effective target density $t$ is defined as the number of polarizable nucleons per cross sectional area [**?**], expressed as $t = N_A \cdot (Z/A)\, d \cdot \rho\, l$, where $N_A$ is the Avogadro constant. The proton and mass number of the butanol molecules ($C_4H_9OH$) are $Z = 10$ and $A = 74$. The dilution or filling factor of the butanol beads is $d = 60\%$. The mass density of butanol at low temperatures is $\rho = 0.94\,\mathrm{g/cm^3}$; the length $l$ of the target is 2 cm. For the transversely polarized butanol target the effective density is then $t = 9.18 \cdot 10^{22}\,/\mathrm{cm^2}$. The target polarization is expected to be approximately $P_T = 70\%$.

The carbon and oxygen in the target material are not polarized, but have a much larger pion photoproduction cross section than the hydrogen. They are not expected to contribute to the asymmetries, but could introduce systematic effects nonetheless. Events on the polarized hydrogen nuclei will be selected mainly using the missing mass technique. Due to the cryostat material around the target volume, charged pions with a momentum below 80 MeV/c and protons with a momentum below 270 MeV/c cannot be detected in the Crystal Ball or TAPS, so detection of the recoiling proton is not possible just above threshold. Direct detection of the $\pi^+$ mesons will be possible for higher photon energies.

For the reaction channel to $\pi^0 p$ the two photons from the decay $\pi^0 \to \gamma\gamma$ will be detected

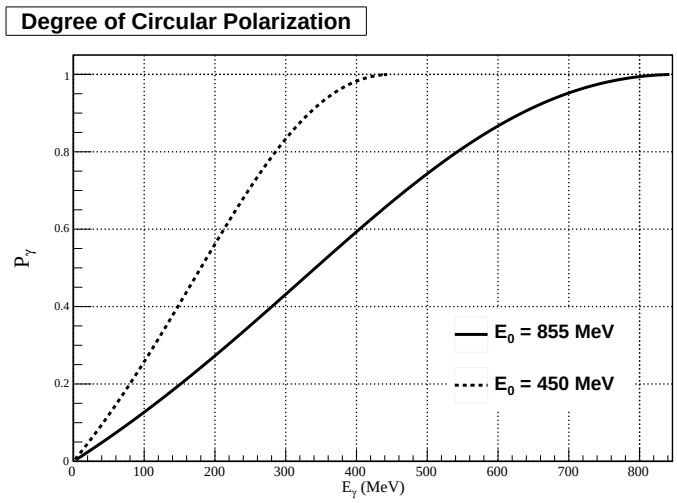


Figure 5: Degree of circular polarization of the photons versus energy. In the region of interest and for an electron beam of 450 MeV, we expect a circular polarization $\Pi_\odot \approx 50\%$ or better.

by the Crystal Ball and/or TAPS (in the forward direction). The detection of protons in the wire chambers will only be useful sufficiently above threshold, when the proton momentum is larger than 270 MeV/c. Therefore, the missing mass and cuts on the opening angle $\theta^*_{\gamma\gamma}$ will be used to separate the contribution of the C and O nuclei. The effectiveness of this procedure is illustrated in Fig. 6 for the missing mass distributions at $\theta^*_\pi = 90^0$ at a photon energies which span the most important energy region that we need precise data. At smaller angles the Carbon contamination increases. We only plan to analyze data for which the Carbon contamination $\leq$0.5. For these values a significant dip is seen between the C and H missing mass peaks. This will limit the pion center of mass angular range to be greater then $60^0$ for energies above $\simeq$ 155 MeV. For lower energies we do not anticipate any angular restrictions. It should also be pointed out that during the experiment we will collect a significant amount of data on the empirical missing mass distributions. This will be accomplished by analyzing the missing mass spectra for different directions of the proton polarization which will enable us to separate the C and H signals. This data will ensure that our C contamination subtractions will be small and accurate.

The detection efficiency of the $\pi^0 p$ reaction channel is expected to be $\epsilon_{\pi^0} = 85\%$. For the estimates below, the geometric detection efficiency is assumed constant although variations with energy and angle of up to 10% can be expected. We should be able to maintain a data acquisition efficiency (live time) of approximately $\epsilon_{DA} = 70\%$.

The estimates below are for a 600 hours production running period. aking into account calibrations and efficiency this corresponds to approximately 6 weeks. We are assuming that there will be an additional general A2 'background run' mode, which will evaluate the contributions from the C and O in the target as well as the walls.

In summary, these are the running conditions used for the event rate estimates in this proposal:

- Electron beam energy: $E_e = 450$ MeV.

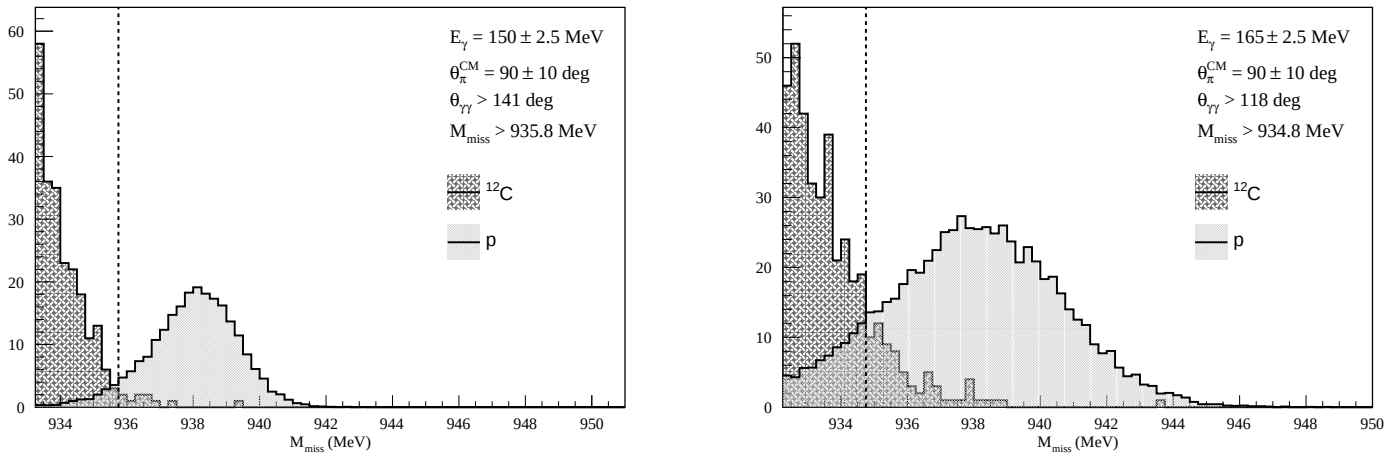


Figure 6: Missing mass distributions for simulated events on H and C at photon energy $k = 150\,\mathrm{MeV}$ and $k = 165\,\mathrm{MeV}$, for a pion center-of-mass angle $\theta_\pi^* = 90^0$. The opening angle $\theta_{\gamma\gamma}^*$ is required to be larger than 141°and 118° for these two cases. The contribution of the H and C events can be well separated.

- Tagged photon energy range: $E_\gamma = 40 - 400\,\mathrm{MeV}$.
- Tagger efficiency: $\epsilon_{tag} = 0.25$ (for a 450 MeV electron beam).
- Photon flux: $\dot{N}_e = 0.5\,\mathrm{MHz/MeV}$.
- Photon polarization: $\Pi_\odot \approx 50\%$.
- Target density: $t = 9.18 \cdot 10^{22}\,/\mathrm{cm}^2$.
- Target polarization: $P_T = 70\%$.
- Detection efficiency: $\epsilon_{\pi^0 p} = 85\%$ and $\epsilon_{\pi^+ n} = 10\%$.
- Data acquisition efficiency: $\epsilon_{DA} = 70\%$.
- Production beam time: $\Delta t = 600\,\mathrm{hours}$.

## 3.2 Estimated Event Rates and Uncertainties

The estimated rate of pions $\dot{N}_\pi$ in an experimental bin with energy width $\Delta k$ and solid angle $\Delta\Omega$ is expressed as

$$\dot{N}_\pi = \epsilon_{tag}\epsilon_\pi\epsilon_{DA} \cdot \dot{N}_e t \cdot \frac{d\sigma}{dk d\Omega}\Delta k \Delta\Omega, \tag{5}$$

where $\dot{N}_e$ is the tagged electron rate. .

Two experimental asymmetries are the focus of this proposal. The target asymmetry between the up and down state of the target polarization(no photon polarization) is defined

as

$$\mathcal{A}_{targ}(\theta_\pi,\varphi_\pi) = \frac{1}{P_T}\frac{N_\uparrow(\varphi_\pi)-N_\downarrow(\varphi_\pi)}{N_\uparrow(\varphi_\pi)+N_\downarrow(\varphi_\pi)} = \mathbf{T}(\theta_\pi)\cos\varphi_\pi = \mathbf{A}(\mathbf{y})\cos\varphi_\pi. \quad (6)$$

The $\cos\varphi$ moment of this asymmetry gives access to the observable $T(\theta_\pi)$.

The asymmetry between the two beam helicity states is defined as

$$\mathcal{A}_{circ}(\theta_\pi,\varphi_\pi) = \frac{1}{\Pi_\odot P_T}\frac{N_+(\varphi_\pi)-N_-(\varphi_\pi)}{N_+(\varphi_\pi)+N_-(\varphi_\pi)} = P_T F(\theta_\pi)\cos\varphi_T = P_T A(\gamma_c,x)\cos\varphi_T, \quad (7)$$

and is sensitive to the observables and $F(\theta_\pi) = A(\gamma_c, x)$.

The uncertainty $\delta\mathcal{A}$ on the experimental asymmetries $\mathcal{A}$ is given by

$$\mathcal{A} = \frac{N_1-N_2}{N_1+N_2}, \quad \text{with } N_1+N_2 = N$$
$$\delta\mathcal{A} \approx \frac{\delta N}{N} = \frac{1}{\sqrt{N}}, \quad (8)$$

where $N = N_\pi$ is again the number of collected pion events.

### 3.3 Reaction Channel $\gamma p \to \pi^0 p$

The measurement of the polarized target asymmetries in the $\gamma p \to \pi^0 p$ reaction is the main focus of this proposal. In the left panel of Fig. 7 we present the estimated statistical uncertainties that we expect to achieve for $\boldsymbol{A(y) \equiv T(\theta)}$. In order to obtain the smallest stastical uncertainty we have averaged the asymmetry over the angular range in $\theta_\pi$ between $60^\circ \to 140^\circ$ (in the center-of-mass system). Since this observable has a $\sin\varphi$ dependence we also averaged over a $\varphi$ ranges between $45^\circ \to 135^\circ$ and $225^\circ \to 315^\circ$; the latter will have the opposite asymmetry.Because of the low cross section just above threshold, the photon energy range between the $\pi^0 p$ and $\pi^+ n$ threshold is lumped together in one bin with $\Delta k \approx 7\,\text{MeV}$. Above the $\pi^+ n$ threshold the points are shown every 1 MeV and typically have statistical uncertainties $\simeq 3\%$ per point. In the right panel of Fig. 7 we show the asymmetry $T$ versus $\theta_\pi$ at a photon energy of 160 MeV with $20^\circ$ bins, and with the same $\varphi$ bins for a photon energy bin of 3 MeV. The curves in Fig. 7 are for ChPT with $\beta = 2.78$ (ChPT) and 3.4 (unitary value) and will be easily distinguished experimentally.

From this data we plan to extract the values of $ImE_{0+}$ using Eq.1. The values with the estimated errors are shown in Fig. 8. It can be seen that the difference between the ChPT and unitary calculations will be easily distinguished. By fitting the known energy dependence in Eq. 1 we anticipate a statistical uncertainty in the parameter $\beta$, and therefore in $a_{cex}(\pi^+ n \to \pi^0 p)$, of $\simeq 1\%$. We anticipate that the systematic error will be $\leq 2\%$ due primarily to our knowledge of the magnitude of the target polarization. If isospin is conserved then $a_{cex}(\pi^+ n \to \pi^0 p) = -a_{cex}(\pi^- p \to \pi^0 n)$; the latter is known experimentally to $\simeq 1.5\%$ [11] from precise measurements on pion hydrogen. The isospin breaking contribution to $a_{cex}(\pi^+ n \to \pi^0 p)$ has been calculated using ChPT to be $\simeq -1.9 \pm 0.8$ %[12]. As can be

seen from the experimental and theoretical errors are reaching the level which can provide us with a significant test of isospin conservation.

At higher energies in the $\pi$N system there have been two independent claims that isospin has been violated in medium-energy (30 to 70 MeV) $\pi$N scattering [37]. Specifically, they showed that the "triangle relationship," which relates the amplitude of charge-exchange scattering ($f(\pi^- p \to \pi^0 n)$) to the elastic scattering amplitudes ($f(\pi^{+(-)} p)$):

$$D \equiv f(\pi^- p \to \pi^0 n) - \frac{1}{\sqrt{2}}(f(\pi^+ p) - f(\pi^- p)) = 0 \tag{9}$$

does not hold. Instead they found

$$\begin{array}{l} D \simeq -0.012 \pm 0.003 \text{ fm} \\ D/f(\pi^- p \to \pi^0 n) \simeq 7\% \end{array} \tag{10}$$

about an order of magnitude larger than has been predicted by ChPT [8]. If true, this is a major discrepancy! However in a recent pion charge exchange experiment reported from TRIUMF [38] the results were consistent with a very small isospin breaking. The main difference between their conclusion and those of Gibbs and Matsinos [37] is due to an experimental discrepancy between two measurements of the pion charge exchange cross section. The proposed measurement is at a level of accuracy that it can test the possibility of an presently unknown mechanism for the isospin violation in the $\pi$N system at the level claimed by Gibbs and Matsinos[37].

The double polarization observable $A(\gamma_c, x) \equiv F(\theta)$ will be measured for the first time in the threshold region in this experiment. This requires a transverse polarized target and a circularly polarized beam. The main information that we expect to obtain from this observable is an accurate measurement of $ReE_{0+}$ and to detect the presence of $d$ waves at low photon energies for the first time. In Fig. 9 we present the difference in the angle $\theta_{F0}$ for which F = 0 as a function of photon energy. It can be seen that there is a small, but significant, difference between the *sp* and *spd* ChPT calculations [28] which levels off $\simeq$ 152 MeV. The fact that $\theta_{F0}$ remains almost constant enhances our ability to measure it. The reason is that we need good statistics and this means we can average the data over energy bins of $\simeq$ 4 MeV. In Fig. 9 we present the estimated errors for an angular measurement for a bin centered at 160 MeV. It is seen that we have an excellent chance of being able to distinguish between the sp and spd calculations.

From the shape of $A(\gamma_c, x) \equiv F(\theta)$ versus $\theta$, which remains fairly constant above $E_\gamma \simeq$ 152 MeV, means that we can integrate the cross section for the range of $\theta_\pi$ from $70^\circ \to 130^\circ$ and obtain a significant difference between the sp and spd calculations and minimize the statistical error. An estimate using this idea has been performed with energy bins of 3 MeV and the result is shown in Fig. 10. It can be seen that this is another way that we have to measure the calculated difference of taking the $d$ waves into account.

## 3.4 Reaction channel $\gamma p \to \pi^+ n$

For the reaction channel to $\pi^+ n$ we hope to detect the $\pi^+$ in the wire chambers around the polarized target when the pion momentum is above 80 MeV/c. The positive pion momentum

as a function of pion center of mass angles is shown in Fig. 11. it is apparent that for a photon energy of 210 MeV or greater that the pion can be detected for all of the angular range.For lower photon energies only part of the angular angular range will be accessible. extent, but at 200 MeV all pions have a high enough momentum. As was stated earlier, the main goal of this proposal is the $\pi^0 p$ channel, and more detailed simulations are planned for the $\pi^+$ channel.

## 3.5 Conclusions

In conclusion we expect that we will be able to measure the time reversal odd asymmetry $\boldsymbol{A(y) \equiv T(\theta)}$ and the double polarization asymmetry $A(\gamma_c, x) \equiv F(\theta)$ for the first time in threshold pion photoproduction. They both require a transverse polarized target which is presently under development. The maximum use will be made of the almost $4\pi$ Crystal Ball plus TAPS detectors. We anticipate a first measurement of the charge exchange scattering length $a_{cex}(\pi^+ n \rightarrow \pi^0 p)$. This can be compared to the experimental value of $a_{cex}(\pi^- p \rightarrow \pi^0 n)$ [11] to provide an isospin test in $\pi$N scattering at the few % level. We also expect to be able to test the unitary and ChPT calculations of $ImE_{0+}$ as well as many other ChPT predictions [26] for a stringent test of the theory and to determine for the first time its convergence limits. In addition we expect to be able to provide a stringent test of the predicted presence of $d$ waves at low energies [28]. Finally we note that this document has focused on the near threshold region for the $\pi^0$ channel. We plan to take data through the $\Delta$ region, and also to include the $\gamma p \rightarrow \pi^+ n$ reaction in the measurement.

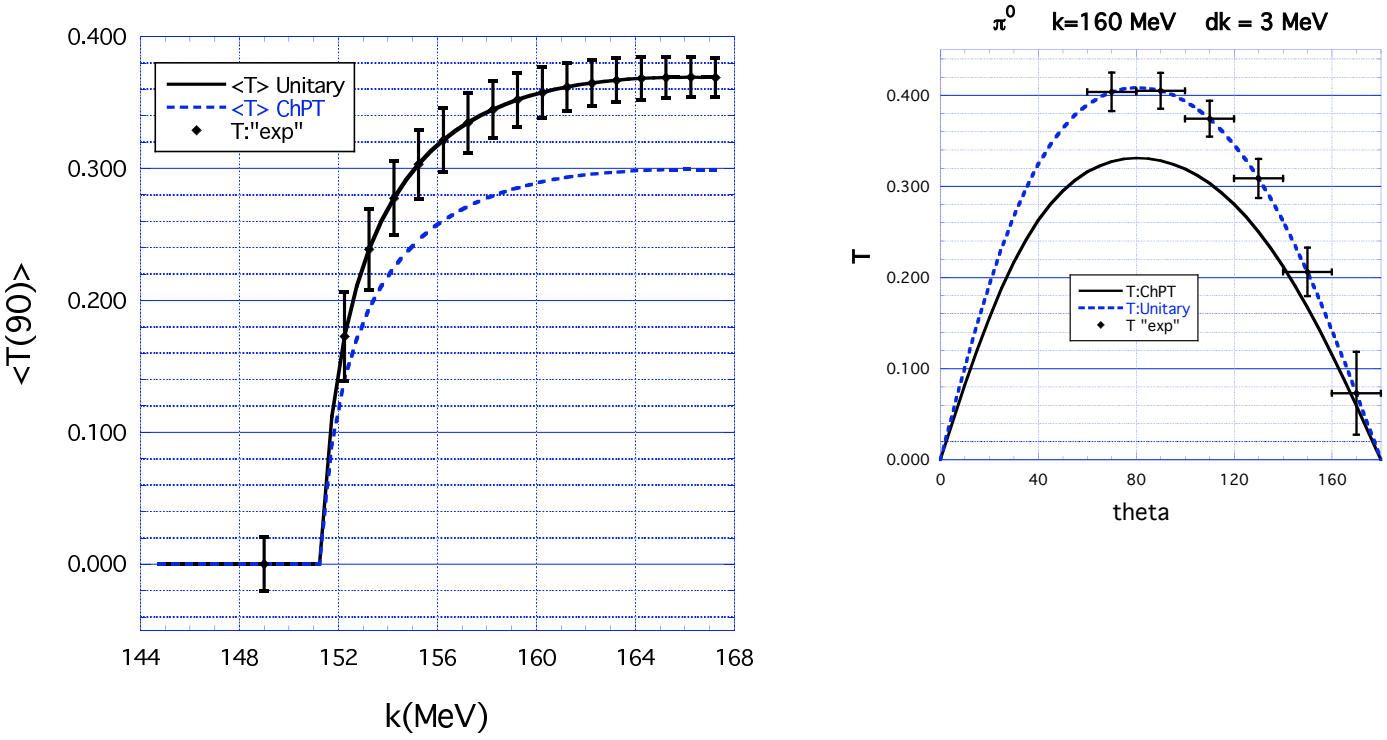


Figure 7: $A(y) \equiv T(\theta)$ for the $\gamma p \to \pi^0 p$ reaction. The points represent the estimated statistical uncertainties. Left panel: The asymmetry versus the photon energy $k$ integrated over an angular region $\theta_\pi$ of $70^\circ \to 140^\circ$ (CM system). The points are shown for 1 MeV wide energy bins (*i.e.* the resolution of the tagger). Right panel: The asymmetry versus the polar angle $\theta_\pi$ for a photon energy $k = 160$ MeV with $20^\circ$ wide bins and an energy bin of 3 MeV. The curves are the ChPT calculations [26] with $\beta = 2.78$ and the unitary value of $\beta = 3.4$ (Eq. 1). See the text for discussion.

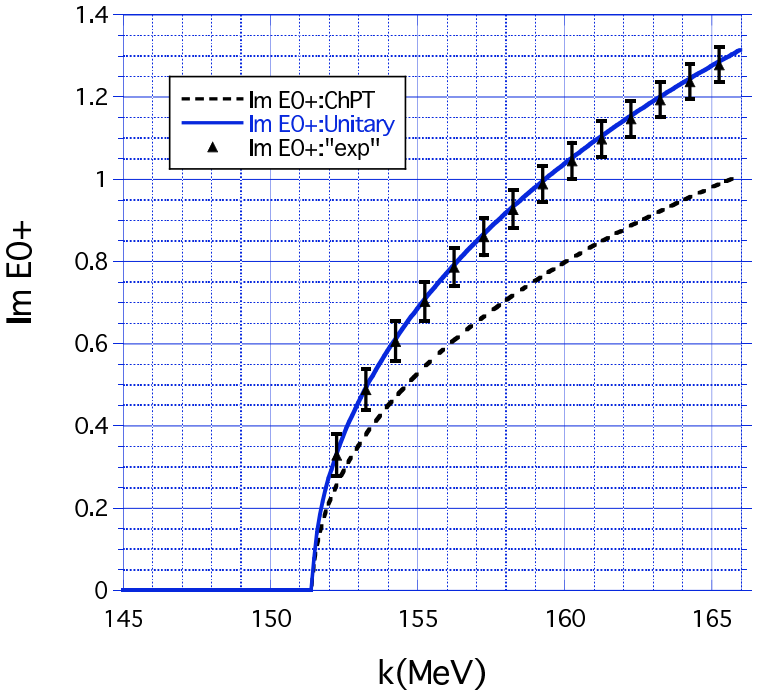


Figure 8: $ImE_{0+}(\gamma p \to \pi^0 p)$. The points, shown every 1 MeV, represent the estimated statistical uncertainty. The curves are the ChPT calculations [26] with $\beta = 2.78$ and the unitary value of $\beta = 3.4$ (Eq. 1). See text for discussion.

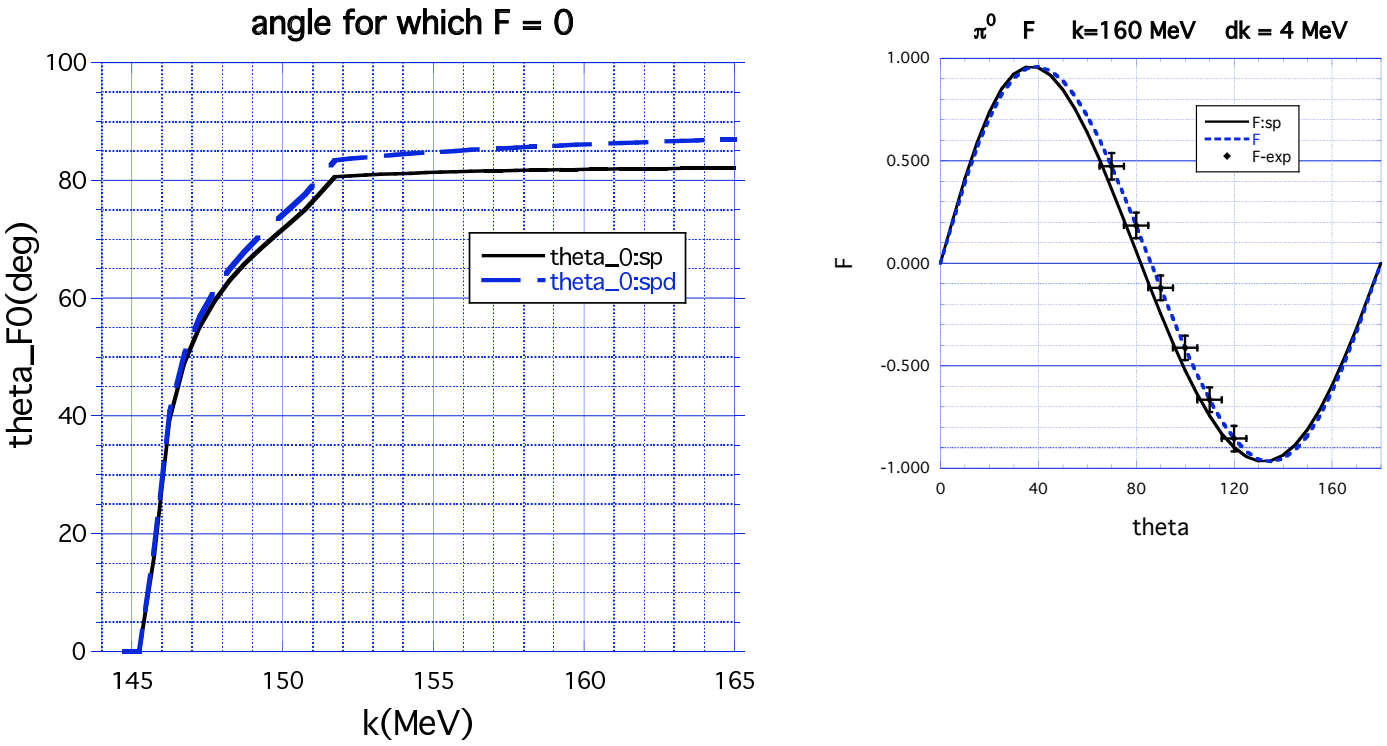


Figure 9: The $A(\gamma_c, x) \equiv F(\theta)$ asymmery. Left panel: The angle $\theta_{F0}$ for which the asymmetry is zero versus the photon energy. Right panel: Asymmetry versus $\theta_\pi$ at a photon energy of 160 MeV. The estimated errors are shown for 20° and four MeV bins. The curves show the *sp* and *spd* ChPT calculations whose low energy parameters have been fit to the data [21]. See text for discussion.

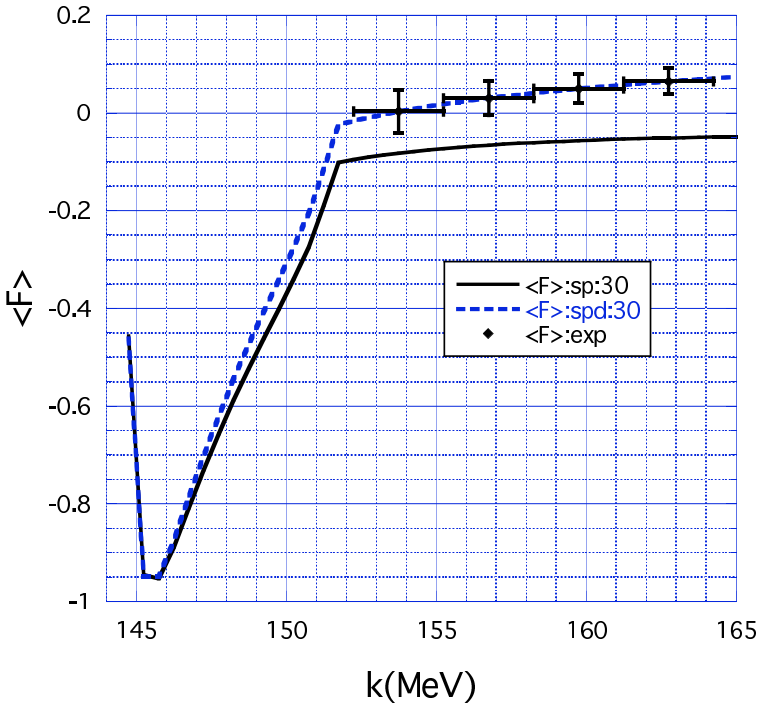


Figure 10: The $A(\gamma_c, x) \equiv F(\theta)$ asymmetry versus photon energy for an angular region $\theta_\pi$ of $70^\circ \rightarrow 140^\circ$ (in the center-of-mass system). The points show the estimated statistical errors for a 3 MeV bin. The curves show the *sp* and *spd* ChPT calculations whose low energy parameters have been fit to the data [21]. See text for discussion.

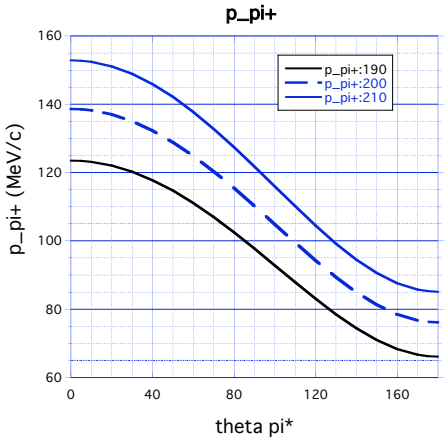


Figure 11: Positive pion momentum for a photon energy of $k = 190\,\mathrm{MeV}$ (solid black), $k = 200\,\mathrm{MeV}$ (dashed blue) and $k = 210\,\mathrm{MeV}$ (solid blue) as a function of polar angle $\theta^*_{\pi^0}$.Pion momentum $\geq$ 80 MeV/c can get out of the target and be detected.

# 4 Event Rate Estimates and Asymmetry Uncertainties

In the following tables the estimated event rates and uncertainties on $T$ and $F$ are summarized for select photon energies. The estimates were obtained for a tagged electron rate $\dot{N}_e = 0.6\,\mathrm{MHz}$, instead of 1 MHz used for the figures.

- Table 2: $k = 160\,\mathrm{MeV}$ energy bin of $\pi^0 p$ channel
- Table 3: $k = 190\,\mathrm{MeV}$ energy bin of $\pi^0 p$ channel

Table 2: Expected event rates and uncertainties for the reaction channel to $\pi^0 p$ with $k = 160\,\mathrm{MeV}$ and $\Delta E_\gamma = 3\,\mathrm{MeV}$.

| $\theta_\pi$ [deg] | $\Delta\Omega$ [sr] | $\frac{d\sigma}{dE_\gamma d\Omega}$ [$\mu$b/sr] | $\dot{N}_\pi$ [1/h] | $T$ | $\delta T$ | $F$ | $\delta F$ |
|---|---|---|---|---|---|---|---|
| 10 | 0.379 | 0.101 | 3.53 | 0.120 | 0.043 | -0.384 | 0.087 |
| 30 | 1.091 | 0.113 | 11.38 | 0.315 | 0.024 | -0.876 | 0.048 |
| 50 | 1.671 | 0.133 | 20.57 | 0.419 | 0.018 | -0.854 | 0.036 |
| 70 | 2.050 | 0.154 | 29.14 | 0.458 | 0.015 | -0.459 | 0.030 |
| 90 | 2.182 | 0.170 | 34.19 | 0.458 | 0.014 | 0.092 | 0.028 |
| 110 | 2.050 | 0.178 | 33.76 | 0.428 | 0.014 | 0.615 | 0.028 |
| 130 | 1.671 | 0.178 | 27.43 | 0.360 | 0.015 | 0.921 | 0.031 |
| 150 | 1.091 | 0.174 | 17.52 | 0.246 | 0.019 | 0.839 | 0.039 |
| 170 | 0.379 | 0.170 | 5.94 | 0.089 | 0.033 | 0.341 | 0.067 |

Table 3: Expected event rates and uncertainties for the reaction channel to $\pi^0 p$ with $k = 190\,\mathrm{MeV}$ and $\Delta E_\gamma = 3\,\mathrm{MeV}$.

| $\theta_\pi$ [deg] | $\Delta\Omega$ [sr] | $\frac{d\sigma}{dE_\gamma d\Omega}$ [$\mu$b/sr] | $\dot{N}_\pi$ [1/h] | $T$ | $\delta T$ | $F$ | $\delta F$ |
|---|---|---|---|---|---|---|---|
| 10 | 0.379 | 0.556 | 19.3 | 0.102 | 0.018 | -0.435 | 0.037 |
| 30 | 1.091 | 0.675 | 67.8 | 0.255 | 0.010 | -0.925 | 0.020 |
| 50 | 1.671 | 0.863 | 132.9 | 0.333 | 0.007 | -0.851 | 0.014 |
| 70 | 2.050 | 1.049 | 198.1 | 0.375 | 0.005 | -0.477 | 0.011 |
| 90 | 2.182 | 1.167 | 234.4 | 0.404 | 0.005 | 0.017 | 0.010 |
| 110 | 2.050 | 1.189 | 224.4 | 0.419 | 0.005 | 0.516 | 0.011 |
| 130 | 1.671 | 1.129 | 173.8 | 0.397 | 0.006 | 0.871 | 0.012 |
| 150 | 1.091 | 1.040 | 104.4 | 0.303 | 0.008 | 0.870 | 0.016 |
| 170 | 0.379 | 0.975 | 34.0 | 0.117 | 0.014 | 0.375 | 0.028 |

# References


[1] E. Amaldi, S. Fubini, and G. Furlan, Pion Electro-production, *Springer Tracts in Modern Physics*, 83 (1979).

[2] G. Höhler, *Pion Nucleon Scattering*, v. 9 of *Landolt-Börnstein*, Springer-Verlag, New York, 1983,

[3] See *e.g.* Dynamics of the Standard Model, J.F.Donoghue, E.Golowich, and B.R.Holstein, Cambridge University Press (1992).

[4] For a review of photo pion physics see the commisioned article for the Annual Reviews of Nuclear Science, A.M.Bernstein,M.W. Ahmed, S. Stave, Y.K.Wu, and H.Weller,arXiv:0902.3650 [nucl-ex] (2009).

[5] V. Bernard and U. Meißner, Ann. Rev. Nucl. Part. Sci **57**, 33 (2007).

[6] V. Bernard, Prog. Part. Nucl. Phys. **60**, 82 (2008).

[7] S.Weinberg,Transactions of the N.Y.Academy of Science Series II 38 (I.I.Rabi Festschrift),185(1977).

[8] N. Fettes and U.G.Meißner, Nucl. Phys. **A693**, 693 (2001), Phys. Rev. **C63**, 045201 (2001).

[9] U.G.Meißner *et al.*, Phys. Lett. **B639**, 478 (2006), Eur. Phys. J. **C41**, 213 (2005), V. Baru *et al.*, arXiv:0711.2743 .

[10] Hadronic Atoms. J. Gasser, V.E. Lyubovitskij, A. Rusetsky, e-Print: arXiv:0903.0257 [hep-ph] (2009)

[11] D. Gotta, AIP conf. Proc., volume 1037,162 (2008).

[12] Martin Hoferichter, Bastian Kubis, Ulf-G. Meissner, e-Print: arXiv:0903.3890 [hep-ph]

[13] S.Weinberg, Phys. Rev. Lett. 17,168(1966)

[14] N. Kroll and M.A.Ruderman, Phys. Rev. **93**, 233 (1954).

[15] For a summary and critique of the early work on low energy theorems for photo-pion physics see G. Ecker and U. Meißner, Comm. Nucl. Part. Phys. **21**, 347 (1995).

[16] S.Weinberg, Physica A96,327(1979). J.Gasser and H.Leutwyler, Ann. Phys.(N.Y.) 158,142(1984), Nucl.Phys. B250, 465 and 517(1985).

[17] For references and the present status of the field see Proceedings of the Workshop on Chiral Dynamics 2006:Theory and Experiment, World Scientific, 2007, M. W. Ahmed, B.R.Holstein, H. Gao, and H. R. Weller, editors.

[18] See e.g. the article by A.M. Bernstein in Proceedings of the Workshop on Chiral Dynamics 2006:Theory and Experiment[17].

[19] R. Beck et al., Phys.Rev.Lett.65,1841(1990).

[20] M.Fuchs et al., *Phys. Lett.*, B368, 20 (1996).

[21] A. Schmidt *et al.*, Phys. Rev. Lett. **87**, 232501 (2001).

[22] . Mainz Experiment A2(6-03)Measurement of the Photon Asymmetry in Neutral Pion Production From the Proton Near Threshold, D. Hornidge, spokesman.

[23] J. C. Bergstrom *et al.*, Phys. Rev. **C55**, 2016 (1997), Phys. Rev. **C58**, 2574 (1998), Phys. Rev. **C57**, 3203 (1998).

[24] E. Korkmaz *et al.*,Phys. Rev. Lett. **83**, 3609 (1999).

[25] V. Bernard, N. Kaiser, and U. G. Meißner, Int. J. Mod. Phys. **E4**, 193 (1995), Nucl. Phys. **B383**, 442 (1992), Phys. Rev. Lett. **74**, 3752 (1995).

[26] V.Bernard, N.Kaiser, and U.G.Meissner, Eur. Phys. J. **A11**, 209 (2001).

[27] V. Bernard, N. Kaiser, and U.-G. Meissner, Phys. Lett. **B383**, 116 (1996).

[28] C. Fernandez-Ramirez, A.M. Bernstein, T.W. Donnelly, Low-Energy D-Wave Effects in Neutral Pion Photoproduction. e-Print: arXiv:0902.3412 [nucl-th] (Feb. 2009)

[29] E. Fermi, Suppl. Nuovo Cimento **2**, 17 (1955). K. M. Watson, Phys. Rev. **95**, 228 (1954).

[30] A. M. Bernstein, Phys. Lett. **B442**, 20 (1998).

[31] B. Ananthanarayan, Phys. Lett. **B634**, 391 (2006).

[32] V. Bernard, N. Kaiser, and Ulf.G. Meißner, *Phys. Lett.* B309, 421 (1993)

[33] S. Kamalov *et al.*, Phys. Lett. **B522**, 27 (2001).

[34] G. Knochlein, D. Drechsel, and L. Tiator, Z. Phys. **A352**, 327 (1995).

[35] D. Drechsel and L.Tiator, J. Phys. G: Nucl, Part. Phys. 18,449(1992). A.S.Raskin and T.W.Donnelly, Annals of Phys.(N.Y.)191, 78(1989).

[36] R. A. Arndt et al. *Phys. Rev. D.*, 43, 2131 (1991), and online SAID program http://gwdac.phys.gwu.edu/.

[37] W.R.Gibbs, Li Ali, and W.B.Kaufmann, Phys. Rev. Lett.,74,3740(1995). E. Matsinos, Phys. Rev.C56, 3014(1997).

[38] Y. Jia *et al.*, Phys. Rev. Lett. **101**, 102301 (2008).

[39] A.M. Bernstein, $\pi N$ Newsletter No. 11, Dec. 1995 , Proceedings of the PANIC Conference, Williamsburg., Va., C.E.Carlson and J.J.Domingo, editors, World Scientific (1996), to be published.